Hindawi Publishing Corporation
Journal of Nanomaterials
Volume 2014, Article ID 518242, 10 pages
http://dx.doi.org/10.1155/2014/518242

Research Article

Nanoscale Zero-Valent Iron for Sulfide Removal from Digested Piggery Wastewater

Sheng-Hsun Chaung,[1] Pei-Fung Wu,[2] Yu-Lin Kao,[3] Weile Yan,[4] and Hsing-Lung Lien[5]

[1] *Department of Environmental Science and Engineering, Tunghai University, Taichung City 407, Taiwan*
[2] *Department of Kinesiology, Health, and Leisure Studies, National University of Kaohsiung, Kaohsiung 811, Taiwan*
[3] *Department of Life Sciences, National University of Kaohsiung, Kaohsiung 811, Taiwan*
[4] *Department of Civil and Environmental Engineering, Texas Tech University, Lubbock, TX 79409, USA*
[5] *Department of Civil and Environmental Engineering, National University of Kaohsiung, Kaohsiung 811, Taiwan*

Correspondence should be addressed to Hsing-Lung Lien; lien.sam@nuk.edu.tw

Received 29 August 2013; Revised 20 January 2014; Accepted 27 January 2014; Published 12 March 2014

Academic Editor: Yitzhak Mastai

The removal of dissolved sulfides in water and wastewater by nanoscale zero-valent iron (nZVI) was examined in the study. Both laboratory batch studies and a pilot test in a 50,000-pig farm were conducted. Laboratory studies indicated that the sulfide removal with nZVI was a function of pH where an increase in pH decreased removal rates. The pH effect on the sulfide removal with nZVI is attributed to the formation of FeS through the precipitation of Fe(II) and sulfide. The saturated adsorption capacities determined by the Langmuir model were 821.2, 486.3, and 359.7 mg/g at pH values 4, 7, and 12, respectively, for nZVI, largely higher than conventional adsorbents such as activated carbon and impregnated activated carbon. The surface characterization of sulfide-laden nZVI using XPS and TGA indicated the formation of iron sulfide, disulfide, and polysulfide that may account for the high adsorption capacity of nZVI towards sulfide. The pilot study showed the effectiveness of nZVI for sulfide removal; however, the adsorption capacity is almost 50 times less than that determined in the laboratory studies during the testing period of 30 d. The complexity of digested wastewater constituents may limit the effectiveness of nZVI. Microbial analysis suggested that the impact of nZVI on the change of microbial species distribution was relatively noticeable after the addition of nZVI.

1. Introduction

Anaerobic digestion of piggery wastewater is capable of producing methane-rich biogas and minimizing the environmental impact caused by the wastewater. The methane-rich biogas is a renewable energy resource that can be used to generate electricity. On the other hand, the Kyoto Protocol has explicitly defined methane as one of the six key greenhouse gases where the global warming potential of methane is 25 times higher than that of carbon dioxide [1]. Thus, the use of methane for electricity generation can not only provide energy but also reduce the methane emission. According to the most recent statistics from the Council of Agriculture in Taiwan, there are 128 pig farms with 5,000 or more swines, an economically sound scale for methane to energy projects [2]. With reference to the methodology based on the Kyoto Protocol mechanisms, this figure represents a potential of over 46,000 megawatt hour (MWh) annually and 800,000 tons of carbon dioxide equivalent (tCO_{2eq}) emission reductions for trading carbon credits.

The biogas consists mainly of methane (50–80%), carbon dioxide (20–50%), and a mix of trace gases including nitrogen (1–4%), hydrogen sulfide (50–5,000 ppm), and others. Hydrogen sulfide is highly corrosive and quickly fractures the cast iron and steel used for many electric generators. Farmers have shown little interest in applying biogas for electricity production because hydrogen sulfide has detrimental effects on the equipment. Therefore, hydrogen sulfide must be removed before biogas can be further utilized.

Several methods for hydrogen sulfide removal have been developed including biological fixation process, liquid-phase absorption with either water or NaOH solution, and adsorption on solids such as activated carbon, iron hydroxide or oxide [3–6]. Among these technologies, adsorption with high adsorption capacity is recognized to be an energy efficient technology for hydrogen sulfide removal. Because of nanotechnology providing high surface areas of nanomaterials, developing a nanoscale adsorbent with high adsorption capacity becomes promising for hydrogen sulfide removal [7, 8].

The nanoscale zero-valent iron (nZVI) represents an important nanotechnology of the environmental remediation that has been developed since 1996 [9]. The nZVI with a particle size of 1–100 nm has been implemented in the field remediation of contaminated groundwater by direct injection technology [10–12]. Extensive studies have indicated the ability of nZVI to remove a wide variety of environmental contaminants including PCBs, chlorinated aliphatic and aromatic hydrocarbons, chlorinated pesticides, heavy metals, and inorganic ions (e.g., nitrate and perchlorate) [8, 9, 13–15]. It has been reported that nZVI has an adsorption capacity towards arsenic ranging from 9 to 174 times greater than conventional ZVI because of its relatively high specific surface areas [16]. The high adsorption capacity of nZVI has been documented for the control of malodorous sulfide-containing compounds generated in biosolids [7, 8].

Though nZVI has been demonstrated to effectively remove sulfide species in the bench scale, the feasibility of nZVI for field applications of sulfide removal has not yet been investigated. In this work, we present here the use of nZVI for effective removal of hydrogen sulfide from the laboratory scale to the field pilot-scale in anaerobically digested piggery wastewater. The pilot test was carried out in a 50,000-pig farm in Taiwan. The objectives of this study include (1) investigating the mechanisms of dissolved sulfide removal by nZVI, (2) exploring the technical feasibility of nZVI for sulfide removal at a pilot scale, and (3) examining the potential impact of nZVI on the microbial community in the anaerobical wastewater.

2. Experimental Methods

2.1. Chemicals and Materials. For the laboratory study, all chemicals were reagent grade or above and used without further purification. Phosphoric acid (85%) and sodium nitrate (99%) were obtained from Scharlau and Showa, respectively. Sodium borohydride ($NaBH_4$, 98%), sodium sulfide, and ferric chloride ($FeCl_3 \cdot 6H_2O$, 98%) were obtained from Aldrich. However, commercial grade chemicals, purchased from Kanto Chemical Co. Inc., Japan, were applied to the pilot test in the field.

2.2. Synthesis of nZVI. In the laboratory studies, synthesis of nZVI was carried out by adding 1 : 1 volume ratio of $NaBH_4$ (0.25 M) into $FeCl_3 \cdot 6H_2O$ (0.045 M) solution. The borohydride to ferric iron ratio was 7.4 times higher than that of the stoichiometric requirement (1). A detailed synthetic procedure has been described elsewhere [17].

Consider the following:

$$4Fe^{3+} + 3BH_4^- + 9H_2O \longrightarrow 4Fe^0 + 3H_2BO_3^- + 12H^+ + 6H_2 \quad (1)$$

The suspension was mixed vigorously under room temperature (22 ± 1°C). The iron particles were magnetically collected and then washed with a large volume of Milli-Q water for at least three times and were used without further treatments unless indicated otherwise.

In the field test, nZVI was produced on site by a batch reactor where 250 g of nZVI was produced in each batch. Approximately 1210 g of $FeCl_3 \cdot 6H_2O$ was dissolved in 10 L water and slowly added into the 10 L $NaBH_4$ aqueous solution (0.45 M). After the completion of the reaction, nZVI was magnetically collected and washed thoroughly with tap water.

It should be pointed out that the characterization of borohydride-synthesized nZVI, which possesses a core-shell morphology with zero-valent iron as the core and iron oxide/hydroxide in the shell has been widely published in many literatures. The detail characterization of nZVI synthesized by the borohydride reduction can be found elsewhere [18–20].

2.3. Batch Experiments. For the study of sulfide removal, experiments were conducted in 150 mL serum bottles containing 1–5 g/L nZVI in 100 mL aqueous solution at 25 ± 1°C. Initial concentrations of sulfide were about 1,000 mg/L. Reaction vessels were placed on a rotary shaker (150 rpm). The solution pH was adjusted at the beginning of the reaction using 1 M HCl or NaOH and monitored periodically throughout the experiment. The adsorption isotherm study was carried out by varying the initial sulfide concentration from 200 to 1,000 mg/L in 100 mL aqueous solution at the nZVI dose of 1.0 g/L at 25 ± 1°C.

2.4. Pilot Studies. Pilot studies were performed in a pig farm in Pingtung, Taiwan. The pig farm has 50,000 pigs that produce 600–700 m^3/d wastewater. The anaerobic digestion tanks have a total volume of 8,640 m^3 resulting in a hydraulic retention time of approximately 15 d. In pilot tests, the anaerobically digested piggery wastewater was fed into a 1,000 L reaction tank containing 1 kg nZVI at the flow rate of 66 L/d to achieve the same hydraulic retention time. A second tank without nZVI was run in parallel under the same conditions (Figure 1). Physicochemical parameters of wastewater quality including temperature, pH, dissolved oxygen (DO), and oxidation-reduction potential (ORP) were measured in the field using a YSI 650 MDS-6600 probe (V2-4 Sonde, YSI Inc.).

2.5. Identification of Anaerobic Bacteria. All the materials of selection and identification of bacteria were purchased from Creative Microbiologicals, Ltd. Taiwan. The fresh specimens were collected from the pig farm in Pingtung, Taiwan. Fresh specimens were inoculated to anaerobic blood agar plate (anBAP) and the anBAP plates were put into MGC

AnaeroPack Jar and cultured at 37°C 24–48 h. According to the morphology of colony growth on anBAP plate, the different colonies were selected and inoculated once again to anBAP plate until one single morphology of colony was cultured. Each fresh single colony was selected in creating slide smear and stained by Gram's stain [21] according to the manufacturer. The fresh single colony was selected and applied to the tube of RapID ANA II system to make an equivalent McFarland turbidity suspension. The entire contents were then transferred into the right upper corner of the panel and incubated at 37°C for 4 h. The anaerobic bacteria were identified by RapID ANA II ID Code.

2.6. Gene Sequencing and Identification. Samples are stored at −20°C for further identification. To clone 16S rRNA, the polymerase chain reaction (PCR) was performed in MyCyclerTM Thermal Cycler (Bio-Rad) according to manual and primers were designed based on NCBI database and the literatures [22, 23]. PCR products were separated on an agarose gel, eluted, and sequenced (Protech Technology Enterprise, Taipei, Taiwan).

2.7. DNA Extraction. Samples (0.1 g) were extracted with Lysis buffer (100 mM Tris-HCl, 100 mM EDTA, 0.75 M sucrose), resuspended, and lysed with 1 μg/μL lysozyme and 0.1 μg/μL achromopeptidase for 30 min at 37°C. Proteinase K (0.2 μg/μL) and 20% sodium dodecyl sulphate (SDS) were added for reaction at 37°C for 2 h; then, 10% cetyl trimethylammonium bromide (CTAB) was added at 60°C for 30 min. Supernatant was collected and reacted with Proteinase K for 30 min at 60°C. Equal amount of phenol/chloroform/isoamyl alcohol (25 : 24 : 1) was added and centrifuged at 14,000 rpm for 5 min. Supernatant was collected, mixed with 700 μL of phenol/chloroform/isoamyl alcohol, and centrifuged for 10 min. Supernatant was mixed with 500 μL of chloroform/isoamyl alcohol and centrifuged for 10 min. Equal amount of isopropanol was added. DNA was precipitated at −20°C. Pellet was washed with iced alcohol (75%), dried, and dissolved in H_2O.

2.8. Analytic Methods. Dissolved sulfide concentrations in the water were analyzed by a spectrophotometer (DR 2700, Hach Co.) using the methylene blue spectrophotometric method. Dissolved iron (Fe(II)) was detected by UV detector at 562 nm by adding ascorbic acid (1% w/v) and ferrozine (3-(2-pyridyl)-5,6-bis (4-phenylsulfonic acid)-1,2,4-triazine) to a 0.45 μm-membrane-filtered sample. Each analysis was performed in duplicate for sulfide and ferrous concentrations.

2.9. Solid Phase Characterization. Surface analysis of nZVI was performed with a high resolution X-Ray photoelectron spectrometer (Scienta ESCA 300 spectrometer). An Al rotating anode serves as the X-ray source generating an Al Kα X-ray beam at 1486.6 eV. The X-ray beam is monochromatized using seven crystals mounted on three Rowland circles. The energy was analyzed using a high-resolution 300 mm mean radius hemispherical electrostatic analyzer and detected by a multichannel plate-CCD camera. Samples that had been previously dried and stored in N_2 glove bag were mounted on a stainless steel stub coated with conductive carbon tape before being transferred to the analysis chamber. Spectra were obtained using a takeoff angle of 90° with respect to the surface plane of the samples. Binding energies of the photoelectrons are correlated to the aliphatic adventitious hydrocarbon C(1s) peak at 284.6 eV.

Figure 1: The 1,000 L reaction tank containing 1 kg nZVI at the flow rate of 66 L/d in the field test.

Morphological and elemental analyses of nZVI were performed by a scanning electron microscope (SEM) (Hitachi S-4300, Hitachi Science Systems, Ltd.) equipped with energy-dispersive X-ray (EDX) at 10 kV. Thermogravimetric analysis (TGA) was conducted using a STA 6000 simultaneous thermal analyzer (PerkinElmer Co.) with a temperature ramp of 20°C/min. The system was purged with air at a flow rate of 20 mL/min.

3. Results and Discussion

3.1. Laboratory Studies. Effectiveness of nZVI for sulfide removal under various pH conditions is illustrated in Figure 2. The initial sulfide concentration was about 1,000 mg/L in an aqueous solution. Approximately 95% of initial sulfide concentration was removed at pH 4. However, the sulfide removal efficiency decreased as pH increased. The oxidation of nZVI leading to generation of Fe(II) is favorable under acidic conditions:

$$Fe^0_{(s)} + 2H_2O \longrightarrow Fe^{2+} + H_{2(g)} + 2OH^- \quad (2)$$

Sulfide readily reacted with Fe(II) to form iron sulfide (FeS) [4, 24]:

$$Fe^{2+} + H_2S \longrightarrow FeS + 2H^+$$
$$Fe^{2+} + HS^- \longrightarrow FeS + H^+ \quad (3)$$

Accordingly, the pH effect on the sulfide removal with nZVI may be attributed to the formation of FeS through the precipitation of Fe(II) and sulfide. To verify the possibility, experiments were conducted to measure the Fe(II) concentrations in the reaction system containing nZVI and

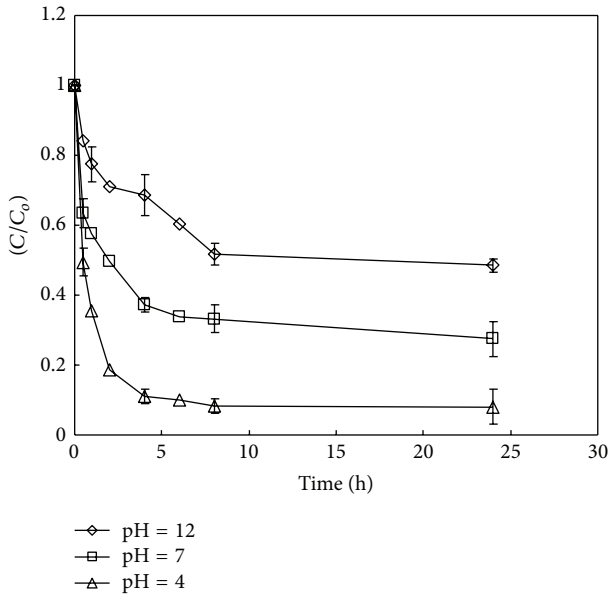

Figure 2: Effect of pH on sulfide removal with nZVI. The nZVI dose was 2.5 g/L.

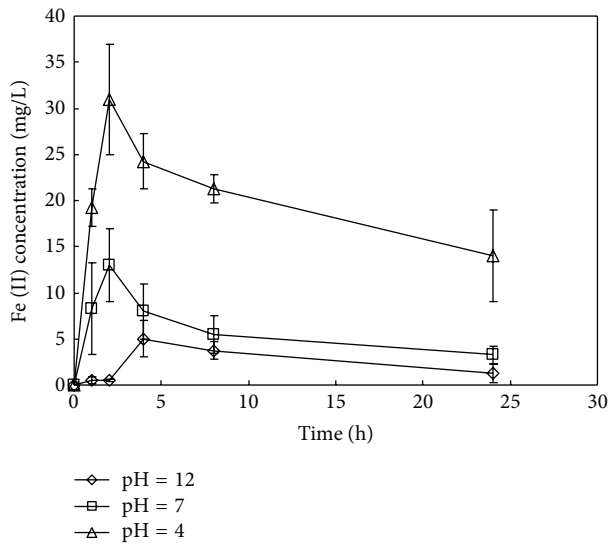

Figure 3: Production of dissolved Fe(II) in the reaction of nZVI with sulfide at different pH. The nZVI dose was 2.5 g/L.

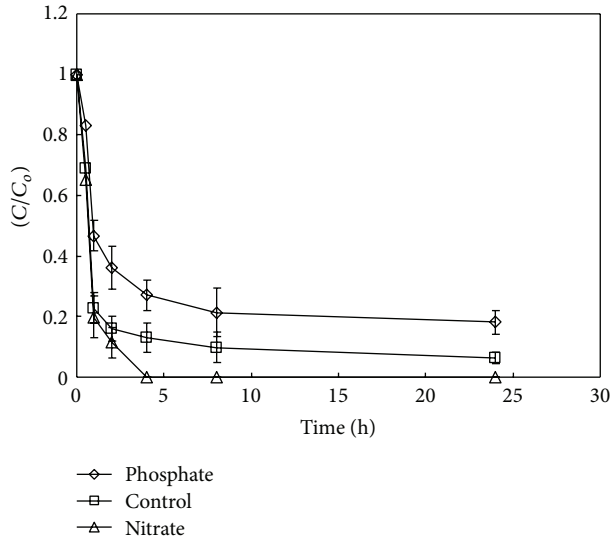

Figure 4: Effect of nitrate and phosphate on sulfide removal with n ZVI at pH 4.0. The nZVI dose was 2.5 g/L. The concentration of nitrate and phosphate was 200 mg/L, respectively.

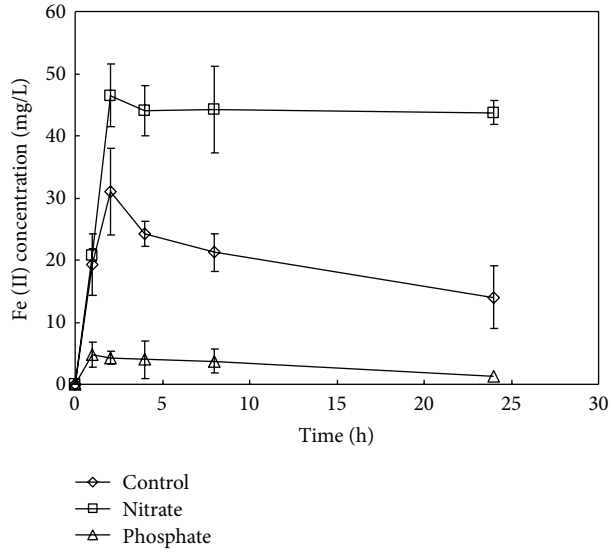

Figure 5: Production of dissolved Fe(II) in the reaction of nZVI with sulfide in the presence of various anions. The nZVI dose was 2.5 g/L. The concentration of nitrate and phosphate was 200 mg/L, respectively.

sulfide at various pH values. As shown in Figure 3, the Fe(II) concentration increased as pH decreased. This is in a good agreement with the theory of FeS formation.

Extensive studies have indicated that nZVI is an effective reagent for nitrate reduction in the aqueous solution under acidic conditions [14, 15]:

$$Fe^0 + NO_3^- + H^+ \longrightarrow Fe^{2+} + NH_4^+ + H_2O \quad (4)$$

Nitrate is reduced to ammonium by nZVI that concurrently releases Fe(II). In other words, nitrate can serve as a promoter of the Fe(II) generation. On the other hand, phosphate is known to inhibit reaction rates of the nitrate reduction by ZVI [25] and to precipitate with Fe(II) to iron phosphate $Fe_3(PO_4)_2$ [26]. Thus, phosphate can act as an Fe(II) scavenger. Figures 4 and 5 show the results for the effects of these anions on the sulfide removal and the Fe(II) formation, respectively, in the presence of nZVI at pH 4. It is clearly observed that an enhanced sulfide removal took place and the Fe(II) concentration increased significantly in the presence of nitrate. However, the sulfide removal efficiency and the Fe(II) concentration declined in the presence of phosphate.

Table 1: Wastewater quality monitored during the period of the pilot test.

	Day 0		Day 1		Day 7		Day 14		Day 30	
	Cont.	Exp.	Cont.	Exp.	Cont.	Exp.	Cont.	Exp.	Cont.	Exp.
T (°C)	29.69	29.61	33.9	35.2	31.27	32.88	28.5	29.47	32.8	31.2
DO (mg/L)	1.0	1.04	0.73	0.63	0.76	0.56	0.45	0.48	0.23	0.41
pH	7.19	7.04	7.15	7.32	7.2	7.35	7.05	7.17	7.2	7.35
ORP (mV)	−384	−372	−388	−376	−312	−322	−325	−270	−398	−350
Fe(II)	4.3	4.1	5.0	19.3	3.25	2.0	4.1	3.25	3.0	3.0

Cont. means the control test; Exp. means the experimental test.

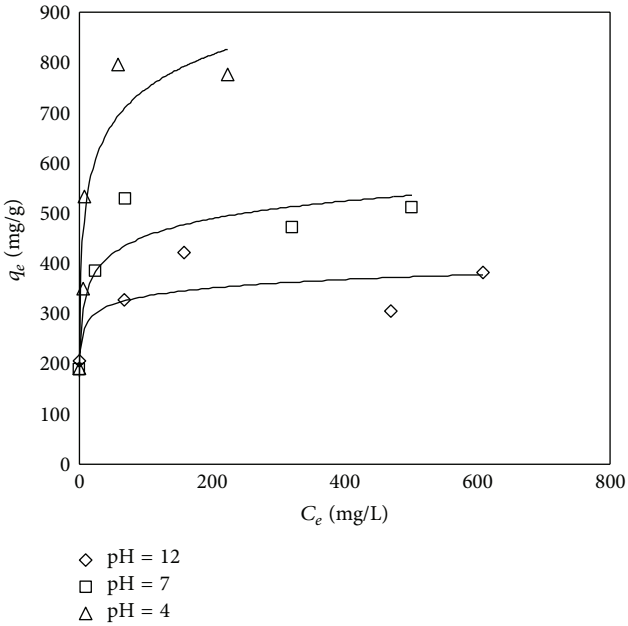

Figure 6: Adsorption isotherms for sulfide reacting with nZVI (1.0 g/L) at 25°C.

The adsorption capacity of nZVI for sulfide removal at various pH values was determined by adsorption isotherm experiments at 25°C. A Langmuir model was tested:

$$q_e = \frac{q_{\max} C_e}{1 + aC_e}, \tag{5}$$

where q_e is the amount of adsorbed sulfide at equilibrium (mg/g), C_e is the equilibrium concentration of dissolved sulfide (mg/L), and $q_{\max}$ and a are Langmuir constants indicating the saturated capacity of nZVI and an energy term, respectively. Figure 6 illustrates the experimental data of the adsorption isotherm for sulfide removal corrected with the Langmuir equation. The coefficients of determination (R^2) were 0.871, 0.885, and 0.689, at pH values 4, 7, and 12, respectively. The saturated adsorption capacities determined by the Langmuir model were 821.2, 486.3, and 359.7 mg/g at pH values 4, 7, and 12, respectively. Compared to the commonly used adsorbents such as virgin activated carbon or impregnated activated carbon, nZVI exhibited a high capacity of sulfide adsorption. For example, the adsorption capacity was estimated to be 62 mg-H_2S/g of 2%-KI impregnated activated carbon in a small pig farm [6] while Yan et al. showed that the capacity of H_2S adsorption varied from 50 to 210 mg-H_2S/g using alkaline activated carbon under different conditions [3].

The adsorption kinetics of sulfide on ZVI was investigated using pseudo-first order and pseudo-second order adsorption equations:

$$\ln \frac{C}{C_o} = -k_1 t,$$
$$\frac{1}{C} = \frac{1}{C_o} + k_2 t, \tag{6}$$

where C is the dissolved sulfide concentration (mg/L), C_o is the initial sulfide concentration (mg/L), k_1 is the rate constant of the pseudo-first order adsorption (1/h), k_2 is the rate constant of the pseudo-second order adsorption (L/mg · h), and t is time (h). Linear regression of the experimental data obtained at pH 4 for these two kinetic models is shown in Figure 6. Values of R^2 were all in the range of 0.95–0.98 for the pseudo-second order model while values of those were 0.78, 0.81, and 0.96 at the nZVI loadings of 1, 2.5, and 5 g/L, respectively, for the pseudo-first order model. Accordingly, the regression results suggested that the sulfide adsorption on nZVI exhibited a second-order kinetic model. This implies that a chemisorption is involved and two distinct sorption sites may be available for the adsorption of sulfide on nZVI [27] (see Figure 7).

3.2. Field Pilot Test. The use of nZVI for *in-situ* full and pilot scale remediation of contaminated groundwater has been implemented around the world including the US, Canada, Czech Republic, Germany, and Taiwan [28]. The removal efficiency of contaminants is generally dependent on the field conditions and the injection amount of nZVI. In this study, a pilot test was conducted to investigate the performance of nZVI for sulfide removal under field conditions in a pig farm. Experiments were carried out in the 1,000 L reaction tank containing 1 kg nZVI at the flow rate of 66 L/d and a second tank without nZVI under the same conditions as control.

Table 1 shows the monitoring results of wastewater quality in the experimental and control tank. The impacts of nZVI on the wastewater quality were insignificant except for the Fe(II) concentration measured at day 1. This is quite different from the result observed in the groundwater remediation with nZVI that influenced the groundwater quality such as

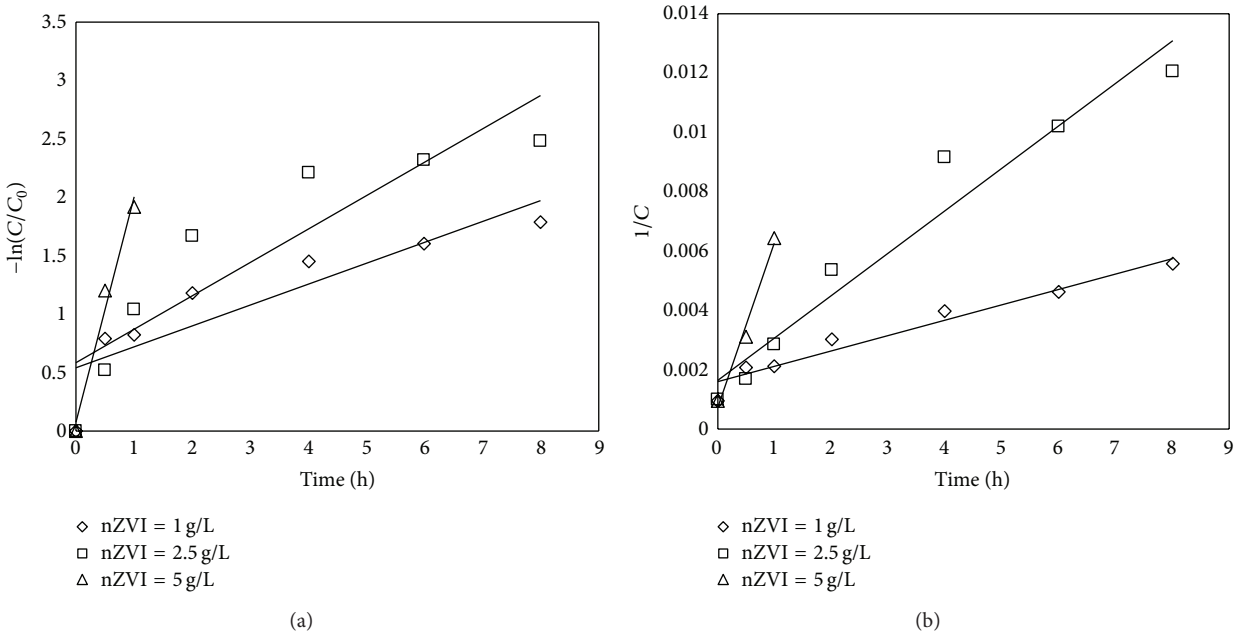

Figure 7: Kinetic models for the adsorption of sulfide on nZVI: (a) pseudo-first order equation and (b) pseudo-second order equation.

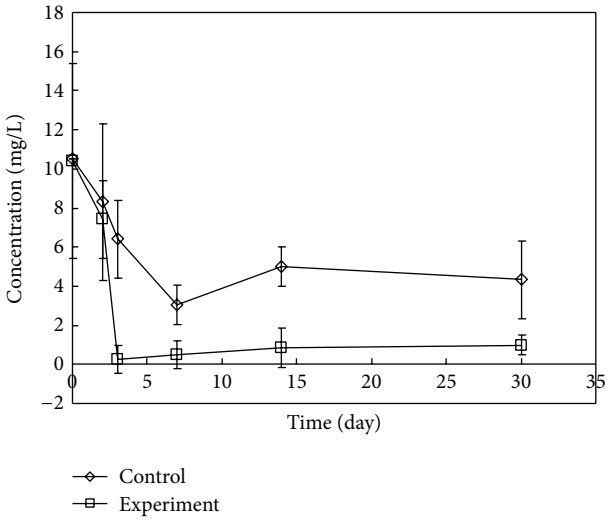

Figure 8: Sulfide removal with nZVI in the pilot study.

pH, ORP, and Fe(II) concentrations largely. For example, the addition of nZVI resulting in an increase in pH and a decrease in ORP in the aqueous system was commonly found both at the laboratory and field studies [8, 11]. It is likely that the anaerobically digested wastewater may contain complex matrices buffering the impact of nZVI on the water quality.

Figure 8 shows the sulfide removal with nZVI in the pilot test during a period of 30 d. The sulfide concentration in the digested wastewater dropped from 8.4 mg/L to around 4.5 mg/L and remained relatively stable in the control tank, while it declined to 0.25 mg/L initially and then gradually increased to 1 mg/L at the end of the test in the experimental tank. This indicates that nZVI is an effective reagent for sulfide removal. However, the total amount of sulfide removed during the pilot test was calculated to be about 10,000 mg, corresponding to the adsorption capacity of 10 mg/g. The adsorption capacity is almost 50 times less than that determined in the laboratory studies at pH 7. According to the results of Figure 8, the breakthrough of sulfide did not actually occur in the pilot study; thus, the adsorption capacity may be underestimated. Nevertheless, the complexity of digested wastewater constituents may limit the effectiveness of nZVI.

The effect of nZVI on the microbial species distribution in the piggery wastewater was examined using gram staining and culture and further confirmed by gene sequencing identification. The study was performed for five months to collect the background information of microbial species before and after the addition of nZVI. The results of the anaerobic organisms identified in the pilot reaction system are listed in Table 2. There were totally 12 species observed before nZVI was added. Among them, only 4 species were identified after the addition of nZVI. In addition, *C. limosum* was only identified after the nZVI addition. The impact of nZVI on the change of the microbial species distribution was relatively noticeable.

Impact of nZVI on the microorganisms in environments has received increased attention since nZVI has been implemented in the full-scale field remediation [29, 30]. Studies have reported that no deleterious microbial effects of nZVI were observed when it was applied to aquifer materials or soil matrix [31–33]. Additionally, nZVI coated with biodegradable polyaspartate stimulated microbial growth [31], which is consistent with a field study where an enhanced biodegradation by surfactant-modified nZVI was found [12]. Fajardo et al. reported a lack of a broad bactericidal effect of nZVI on the bulk soil microbial community; however, significant

Table 2: Microbial species distribution before and after the addition of nZVI.

Anaerobic microbial species	Before	After
C. tertium	+	+
Camp. gracilis	+	−
Ps. tetradius	+	−
C. perfringens	+	+
C. baratii	+	+
C. botulinum	+	−
C. septicum	+	−
Ps. prevotii	+	−
Prop. acnes	+	−
Wolinella sp.	+	+
Gemella morbillorum	+	−
F. mortiferum	+	−
C. limosum	−	+

"+": identified; "−": nonidentified.

changes in the structure and composition of the soil bacteria population were detected in the presence of nZVI [33]. On the contrary, other studies showed divergent results. For example, Lee et al. found that nZVI had a strong bactericidal effect on *E. coli* under deaerated conditions [34] while complete inactivation of *B. subtilis var. niger* and *P. fluorescens* by nZVI (10 g/L) was observed with vigorous shaking under aerobic conditions [35]. It should be pointed out that our study examined only the identification of microbial species. There is a need to attain quantitative information of microorganisms in order to better understand the impact of nZVI on the environments.

3.3. Removal Mechanisms. Surface characterization of nZVI using EDX, TGA, and XPS was conducted to gain insight into the mechanism of sulfide removal with nZVI. The EDX analysis indicated a precipitate of sulfur species on the surface of nZVI. The TGA analysis of the sulfide-laden nZVI was performed over the temperature range 105–600°C in air (Figure 9). The first event of weight loss occurring at 195°C is caused essentially by water vaporization from the samples. The weight gain occurring at 300°C can be attributed to the transformation of FeS to $FeSO_4$ [36], while another weight gain appearing at 550°C is likely due to the oxidation of iron to hematite [37]. The results of TGA analysis suggested that the formation of FeS took place on the nZVI surface when nZVI reacted with sulfide.

Figure 10 presents the S 2p survey of nZVI in reactions with and without sulfide after 17 d. The sulfur spectra were fitted by using doublets $2p_{1/2}$ and $2p_{3/2}$ with the same full width at half maximum (FWHM) separated by a spin-orbit splitting of 1.2 eV. The S $2p_{1/2}$ peak intensity was constrained to be half that of S $2p_{3/2}$ peak. It was decomposed into five subsets of doublets with the $2p_{3/2}$ peak binding energies at 161.3, 162, 163.4, 166.9, and 168.4 eV. These five peaks can be assigned to monosulfide (S^{2-}), disulfide (S_2^{2-}), polysulfide (S_n^{2-}), sulfite (SO_3^{2-}), and sulfate (SO_4^{2-}), respectively [38].

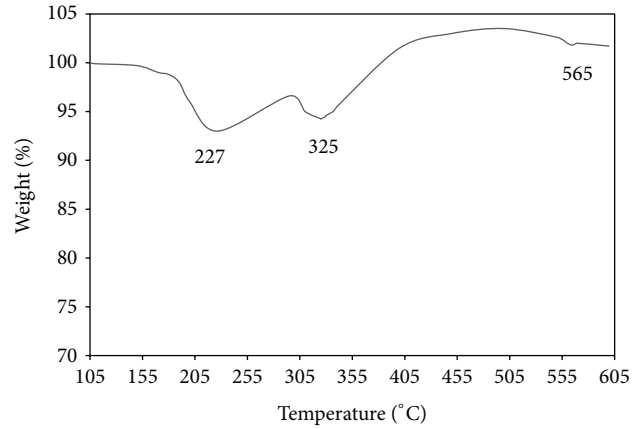

Figure 9: Thermogravimetric plot of sulfide-laden nZVI heated at a rate of 20°C/min in 20 mL/min air flow.

The areas of the fitting curves suggested that approximately 25.8% of sulfur on the surface existed as monosulfide, 22.4% as disulfide, 35.9% as polysulfide, 8% as sulfite, and 7.9% as sulfate. Li et al. have reported the use of nZVI for sulfide removal [9]. The XPS analysis of nZVI after 24 h of reaction with hydrogen sulfide indicated that approximately 36% of sulfur on the surface existed as monosulfide and 64% as disulfide. In comparison to this study, it was found that monosulfide and disulfide were significantly decreased, whereas polysulfide became a dominant species when a longer reaction period was conducted. This suggests that a transformation of disulfide to polysulfide, which is a favorable process for the enhanced adsorption of sulfide, may be involved in the reaction of nZVI with sulfide.

Hydrosulfide that was anoxically converted into thiosulfate and polysulfides by iron/cerium oxide hydroxide has been found at pH 8.0–11.0 under the ambient pressure and temperature conditions [39]. The nZVI has a core-shell structure containing a metallic core with a highly reducing characteristic and a thin amorphous iron (oxy)hydroxide layer promoting oxidation reactions [8, 40]. The formation of polysulfides was attributed to an iron-polysulfide surface complex at the iron (oxy)hydroxide surface [39]. In addition, the second-order kinetic behavior for sulfide adsorption with nZVI was observed in this study. Taken together, the reaction mechanism of sulfide removal with nZVI can be considered as a homogeneous-heterogeneous process. The homogeneous process involves the iron dissolution to Fe(II) that reacts with dissolved sulfide to form the FeS precipitate on the surface of nZVI. The surface associated sulfide can further react with H_2S and form $\equiv FeS_2$:

$$\equiv FeS + H_2S \longrightarrow FeS_2 + H_2 \quad (7)$$

where the symbol ≡ denotes the reactive sites at the nZVI surface. This is consistent with the studies reported by Yan et al. [8]. On the other hand, this work provides new evidence for the formation of polysulfide, an aged product of nZVI reacting with sulfide. The formation of disulfide and polysulfide suggests that the iron-polysulfide surface complex may take

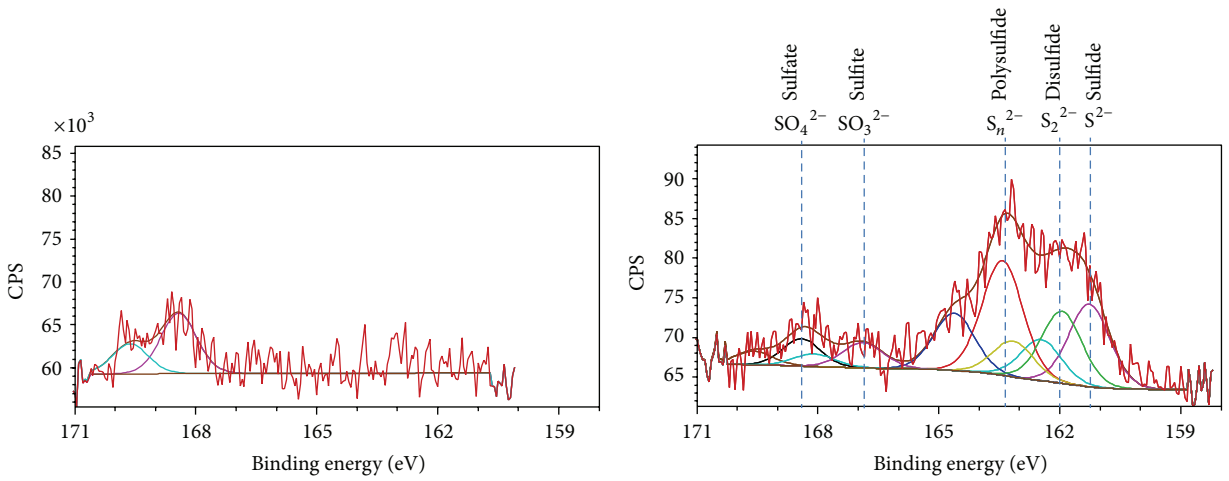

Figure 10: S 2p HR-XPS spectrum of nZVZI reacted (a) without sulfide over 17 d and (b) with sulfide over 17 d.

place at the iron (oxy)hydroxide surface of nZVI, which is another process for sulfide removal by nZVI.

3.4. Cost Effectiveness of nZVI. The cost for synthesis of 1 g nZVI using the sodium borohydride reduction is about 1 USD based on the estimation of cost of industrial grade chemicals. Sodium borohydride is an expensive reductant, which accounts for nearly 99% of the total cost of borohydride-produced nZVI. Therefore, it is difficult to apply borohydride-produced nZVI for sulfide removal in the real-world situation. Nevertheless, we have found that the elemental aluminum rod is a low-cost reductant that may be used to synthesize nZVI. The total cost of 1 g aluminum-produced nZVI is estimated to be 0.01 USD, which is more competitive to be applied to the wastewater treatment in real conditions.

4. Conclusions

Nanoscale zero-valent iron (nZVI) developed since 1996 represents an important nanotechnology for environmental protection and remediation. We have applied nZVI for dissolved sulfide removal and performed a field pilot test in a 50,000-pig farm to treat dissolved sulfide in anaerobically digested wastewater. The field test suggests that nZVI is an effective reagent for sulfide removal; however, the adsorption capacity is calculated to be about 10 mg/g, almost 50 times less than that determined in the laboratory studies. The complexity of digested wastewater constituents may limit the effectiveness of nZVI. The impact of nZVI on microbial species distribution was relatively noticeable. Further studies are needed to better characterize the impact of nZVI on the environments. Laboratory studies revealed that the reaction mechanism of sulfide removal with nZVI can be considered as a homogeneous-heterogeneous process. The dissolved Fe(II) reacts with sulfide to form the FeS precipitate on the surface of nZVI and an iron-polysulfide surface complex may be involved to form disulfide and polysulfide.

Conflict of Interests

The authors declare that there is no conflict of interests regarding the publication of this paper.

Acknowledgments

The authors would like to thank the National Science Council (NSC) and Environmental Protection Administration (EPA), Taiwan, R.O.C., for the financial support under Grant nos. NSC 98-2622-E-390-003-CC3 and 99-2622-E-390-002-CC3 and EPA-101-U1U1-02-101, respectively. Laboratory assistance provided by Mr. Chia-Wei Yang, Ms. Nien-Chun Hsieh, and Mr. Kuo-Ming Chiang are greatly appreciated.

References

[1] United Nations, *Kyoto Protocol to the United Nations Framework Convention on Climate Change*, United Nations, New York, NY, USA, 1998.

[2] Council of Agriculture, *Agriculture Statistics Yearbook 119*, Council of Agriculture, Executive Yuan, Taiwan, 2010.

[3] R. Yan, D. T. Liang, L. Tsen, and J. H. Tay, "Kinetics and mechanisms of H2S adsorption by alkaline activated carbon," *Environmental Science and Technology*, vol. 36, no. 20, pp. 4460–4466, 2002.

[4] A. H. Nielsen, P. Lens, J. Vollertsen, and T. Hvitved-Jacobsen, "Sulfide-iron interactions in domestic wastewater from a gravity sewer," *Water Research*, vol. 39, no. 12, pp. 2747–2755, 2005.

[5] Y. H. Xiao, S. D. Wang, D. Y. Wu, and Q. Yuan, "Catalytic oxidation of hydrogen sulfide over unmodified and impregnated activated carbon," *Separation and Purification Technology*, vol. 59, no. 3, pp. 326–332, 2008.

[6] S. Pipatmanomai, S. Kaewluan, and T. Vitidsant, "Economic assessment of biogas-to-electricity generation system with H_2S removal by activated carbon in small pig farm," *Applied Energy*, vol. 86, no. 5, pp. 669–674, 2009.

[7] X. Q. Li, D. G. Brown, and W. X. Zhang, "Stabilization of biosolids with nanoscale zero-valent iron (nZVI)," *Journal of Nanoparticle Research*, vol. 9, no. 2, pp. 233–243, 2007.

[8] W. L. Yan, A. A. Herzing, C. J. Kiely, and W. Zhang, "Nanoscale zero-valent iron (nZVI): aspects of the core-shell structure and reactions with inorganic species in water," *Journal of Contaminant Hydrology*, vol. 118, no. 3-4, pp. 96–104, 2010.

[9] X. Q. Li, D. W. Elliott, and W. X. Zhang, "Zero-valent iron nanoparticles for abatement of environmental pollutants: materials and engineering aspects," *Critical Reviews in Solid State and Materials Sciences*, vol. 31, no. 4, pp. 111–122, 2006.

[10] M. J. Borda, R. Venkatakrishnan, and F. Gheorghiu, "Status of nZVI technology: lessons learned from north American and international field implementations," in *Environmental Applications of Nanoscale and Microscale Reactive Metal Particles*, C. L. Geiger and K. M. Carvalho-Knighton, Eds., ACS Symposium Series 1027, pp. 219–232, American Chemical Society, Washington, DC, USA, 2009.

[11] Y. T. Wei, S. C. Wu, C. M. Chou, C. H. Che, S. M. Tsai, and H. L. Lien, "Influence of nanoscale zero-valent iron on geochemical properties of groundwater and vinyl chloride degradation: a field case study," *Water Research*, vol. 44, no. 1, pp. 131–140, 2010.

[12] Y. T. Wei, S. C. Wu, S. W. Yang, C. H. Che, H. L. Lien, and D. H. Huang, "Biodegradable surfactant stabilized nanoscale zero-valent iron for in situ treatment of vinyl chloride and 1,2-dichloroethane," *Journal of Hazardous Materials*, vol. 211-212, pp. 373–380, 2012.

[13] A. Taghavy, J. Costanza, K. D. Pennell, and L. M. Abriola, "Effectiveness of nanoscale zero-valent iron for treatment of a PCE-DNAPL source zone," *Journal of Contaminant Hydrology*, vol. 118, no. 3-4, pp. 128–142, 2010.

[14] A. Ryu, S. Jeong, A. Jang, and H. Choi, "Reduction of highly concentrated nitrate using nanoscale zero-valent iron: effects of aggregation and catalyst on reactivity," *Applied Catalysis B*, vol. 105, no. 1-2, pp. 128–135, 2011.

[15] T. Suzuki, M. Moribe, Y. Oyama, and M. Niinae, "Mechanism of nitrate reduction by zero-valent iron: equilibrium and kinetics studies," *Chemical Engineering Journal*, vol. 183, pp. 271–277, 2012.

[16] C. Yuan and H. L. Lien, "Removal of arsenate from aqueous solution using nanoscale iron particles," *Water Quality Research Journal of Canada*, vol. 41, no. 2, pp. 210–215, 2006.

[17] H. L. Lien and W. X. Zhang, "Nanoscale Pd/Fe bimetallic particles: catalytic effects of palladium on hydrodechlorination," *Applied Catalysis B*, vol. 77, no. 1-2, pp. 110–116, 2007.

[18] J. T. Nurmi, P. G. Tratnyek, V. Sarathy et al., "Characterization and properties of metallic iron nanoparticles: spectroscopy, electrochemistry, and kinetics," *Environmental Science and Technology*, vol. 39, no. 5, pp. 1221–1230, 2005.

[19] J. E. Martin, A. A. Herzing, W. Yan et al., "Determination of the oxide layer thickness in core-shell zerovalent iron nanoparticles," *Langmuir*, vol. 24, no. 8, pp. 4329–4334, 2008.

[20] X. Li and W. X. Zhang, "Sequestration of metal cations with zerovalent iron nanoparticles: a study with high resolution x-ray photoelectron spectroscopy (HR-XPS)," *Journal of Physical Chemistry C*, vol. 111, no. 19, pp. 6939–6946, 2007.

[21] H. C. J. Gram, "The differential staining of Schizomycetes in tissue sections and in dried preparations," *Fortschitte der Medicin*, vol. 2, pp. 185–189, 1884.

[22] T. Barry, C. M. Glennon, L. K. Dunican, and F. Gannon, "The 16 s/23 s ribosomal spacer region as a target for DNA probes to identify eubacteria," *PCR Methods and Applications*, vol. 1, no. 2, p. 149, 1991.

[23] P. Fach, S. Perelle, F. Dilasser et al., "Detection by PCR-enzyme-linked immunosorbent assay of Clostridium botulinum in fish and environmental samples from a coastal area in Northern France," *Applied and Environmental Microbiology*, vol. 68, no. 12, pp. 5870–5876, 2002.

[24] D. Rickard and G. W. Luther III, "Chemistry of iron sulfides," *Chemical Reviews*, vol. 107, no. 2, pp. 514–562, 2007.

[25] C. Su and R. W. Puls, "Nitrate reduction by zerovalent iron: effects of formate, oxalate, citrate, chloride, sulfate, borate, and phosphate," *Environmental Science and Technology*, vol. 38, no. 9, pp. 2715–2720, 2004.

[26] O. Gutierrez, D. Park, K. R. Sharma, and Z. Yuan, "Iron salts dosage for sulfide control in sewers induces chemical phosphorus removal during wastewater treatment," *Water Research*, vol. 44, no. 11, pp. 3467–3475, 2010.

[27] Y.-S. Ho, "Review of second-order models for adsorption systems," *Journal of Hazardous Materials*, vol. 136, no. 3, pp. 681–689, 2006.

[28] C. Macé, S. Desrocher, F. Gheorghiu et al., "Nanotechnology and groundwater remediation: a step forward in technology understanding," *Remediation Journal*, vol. 16, no. 2, pp. 23–33, 2006.

[29] K. D. Grieger, A. Fjordbøge, N. B. Hartmann, E. Eriksson, P. L. Bjerg, and A. Baun, "Environmental benefits and risks of zero-valent iron nanoparticles (nZVI) for in situ remediation: risk mitigation or trade-off?" *Journal of Contaminant Hydrology*, vol. 118, no. 3-4, pp. 165–183, 2010.

[30] R. Dinesh, M. Anandaraj, V. Srinivasan, and S. Hamza, "Engineered nanoparticles in the soil and their potential implications to microbial activity," *Geoderma*, vol. 173-174, pp. 19–27, 2012.

[31] T. L. Kirschling, K. B. Gregory, E. G. Minkley Jr., G. V. Lowry, and R. D. Tilton, "Impact of nanoscale zero valent iron on geochemistry and microbial populations in trichloroethylene contaminated aquifer materials," *Environmental Science and Technology*, vol. 44, no. 9, pp. 3474–3480, 2010.

[32] L. G. Cullen, E. L. Tilston, G. R. Mitchell, C. D. Collins, and L. J. Shaw, "Assessing the impact of nano- and micro-scale zerovalent iron particles on soil microbial activities: particle reactivity interferes with assay conditions and interpretation of genuine microbial effects," *Chemosphere*, vol. 82, no. 11, pp. 1675–1682, 2011.

[33] C. Fajardo, L. T. Ortíz, M. L. Rodríguez-Membibre, M. Nande, M. C. Lobo, and M. Martin, "Assessing the impact of zero-valent iron (ZVI) nanotechnology on soil microbial structure and functionality: a molecular approach," *Chemosphere*, vol. 86, no. 8, pp. 802–808, 2012.

[34] C. Lee, Y. K. Jee, I. L. Won, K. L. Nelson, J. Yoon, and D. L. Sedlak, "Bactericidal effect of zero-valent iron nanoparticles on Escherichia coli," *Environmental Science and Technology*, vol. 42, no. 13, pp. 4927–4933, 2008.

[35] M. Diao and M. Yao, "Use of zero-valent iron nanoparticles in inactivating microbes," *Water Research*, vol. 43, no. 20, pp. 5243–5251, 2009.

[36] G. Hu, K. Dam-Johansen, S. Wedel, and J. P. Hansen, "Decomposition and oxidation of pyrite," *Progress in Energy and Combustion Science*, vol. 32, no. 3, pp. 295–314, 2006.

[37] S. M. Ponder, J. G. Darab, J. Bucher et al., "Surface chemistry and electrochemistry of supported zerovalent iron nanoparticles in the remediation of aqueous metal contaminants," *Chemistry of Materials*, vol. 13, no. 2, pp. 479–486, 2001.

[38] M. Mullet, S. Boursiquot, M. Abdelmoula, J. Génin, and J. Ehrhardt, "Surface chemistry and structural properties of mackinawite prepared by reaction of sulfide ions with metallic iron," *Geochimica et Cosmochimica Acta*, vol. 66, no. 5, pp. 829–836, 2002.

[39] C. F. Petre, *Alkaline oxidation of hydrosulfide and methyl mercaptide by iron/cerium oxide-hydroxide in presence of dissolved oxygen. Possible application for removal of Total Reduced Sulfur (TRS) emissions in the Pulp & Paper industry [Ph.D. thesis]*, Université Laval, Québec, Canada, 2007.

[40] M. A. V. Ramos, Y. Weile, X. Li, B. E. Koel, and W. Zhang, "Simultaneous oxidation and reduction of arsenic by zero-valent iron nanoparticles:Understanding the significance of the core-shell structure," *Journal of Physical Chemistry C*, vol. 113, no. 33, pp. 14591–14594, 2009.